

## Magnetic and Nuclear-Resonance Properties of Single-Crystal Scandium†

J. W. ROSS,\* F. Y. FRADIN, L. L. ISAACS, AND D. J. LAM

*Argonne National Laboratory, Argonne, Illinois 60439*

(Received 28 January 1969)

Magnetic-susceptibility, magnetic-anisotropy, and nuclear-magnetic-resonance measurements were performed on single-crystal scandium samples from 4.2 to 300°K. The susceptibility of single-crystal scandium is greater along the  $a$  axis than along the  $c$  axis. The nuclear relaxation rate  $(T_1T)^{-1}$  has a  $\sin^2\theta$  dependence on the angle between the static magnetic field and the crystallographic  $c$  axis. The orbital hyperfine interaction is the major contribution to the relaxation rate. From the experimental results, values are estimated for the electronic density of states, the average fractional  $s$  character, the average fractional admixture coefficients for  $d$  electrons at the Fermi surface, and the orbital paramagnetism.

### INTRODUCTION

THE magnetic susceptibility  $\chi$  of polycrystalline scandium has been measured by several groups.<sup>1-6</sup> Large differences in the values of  $\chi$  and in the temperature dependence of  $\chi$  are noted among the results. Various authors have attributed the discrepancies to differences in impurity content of the individual samples. Recently, Wohleben<sup>7</sup> found that the  $\chi$  of scandium in the temperature range of 0.3 to 300°K was also dependent on crystal imperfections. The susceptibility of a scandium single crystal has been measured over the temperature range of 77-1100°K by Chechernikov *et al.*<sup>8</sup> They reported that  $\chi_c$  (magnetic field parallel to  $c$  axis) is greater than  $\chi_a$  (magnetic field perpendicular to  $c$  axis) and both follow a Curie-Weiss temperature dependence.

Nuclear-magnetic-resonance (NMR) studies provide a bridge between the macroscopic and microscopic magnetic properties. The first NMR studies on metallic scandium were reported by Blumberg *et al.*<sup>9</sup> Barnes and co-workers<sup>10</sup> reported room-temperature results of the anisotropic Knight shifts and the quadrupole interactions of Sc<sup>45</sup> in polycrystalline scandium. The nuclear spin-lattice relaxation time  $T_1$  of Sc<sup>45</sup> in scandium metal was reported by Masuda<sup>11</sup> and by Narath

and Fromhold.<sup>12</sup> The several sources of data agree reasonably well on the Knight-shift value, but the relaxation-time values show considerable scatter.

In the subsequent parts of this paper, we report the results of our studies on (a) the magnetic susceptibility of polycrystalline and single-crystal scandium and (b) the magnetic anisotropy, anisotropic Knight shifts, and spin-lattice relaxation time<sup>13</sup> of single-crystal scandium.

A distinct advantage of this investigation is that all of the measurements were carried out either on the same specimen or specimens prepared in an identical manner, from the same batch of scandium. In the different types of measurements, this precaution limits the effect of impurities by maintaining the same kind and amount of impurities.

### EXPERIMENTAL DETAILS

The scandium employed in this study was purchased from United Mineral and Chemical Corporation (Johnson Matthey and Co., Lot No. M234). Polycrystalline samples were prepared by levitation melting and were cast into a pin-shaped copper mold. Specimens for the susceptibility measurements were spark-cut from the casting. Two single crystals of scandium were prepared at Argonne, and two single crystals were purchased from Koch Light Laboratories, United Kingdom. One single crystal (ANL-I) was prepared by annealing arc-melted buttons at 1050°C for 15 h. Another single crystal (ANL-IV) was spark-cut from an annealed ingot prepared by levitation melting and heat treated in the same manner as ANL-I. The single-crystal sample for the NMR studies was prepared by spark-cutting a portion of the ANL-IV crystal into slices 0.009 in. thick and stacking the slices alternately with 0.001-in.-thick mica insulation. A powder sample for NMR studies was prepared by filing the button from which we obtained the ANL-IV single crystal. The mass spectroscopic analyses of the samples studied are given in Table I.

The experimental apparatus and the methods employed for the magnetic-susceptibility and the magnetic-

† Work performed under the auspices of the U. S. Atomic Energy Commission.

\* Present address: Physical Laboratories, the University of Manchester, Manchester, England.

<sup>1</sup> H. Bommer, *Z. Elektrochem.* **45**, 357 (1939).

<sup>2</sup> V. K. Iya, *J. Rech. Centre Natl. Rech. Sci. Lab. Bellevue (Paris)* **35**, 91 (1956).

<sup>3</sup> V. I. Chechernikov, I. Pop, O. P. Naumkin, and V. F. Terekhova, *Zh. Eksperim. i Teor. Fiz.* **44**, 387 (1963) [English transl.: *Soviet Phys.—JETP* **17**, 265 (1963)].

<sup>4</sup> V. N. Volkenshteyn and E. V. Galoshina, *Fiz. Metal. i Metaloved.* **16**, 298 (1963).

<sup>5</sup> W. E. Gardner and J. Penfold, *Phil. Mag.* **11**, 549 (1963).

<sup>6</sup> H. Kobayashi, *J. Phys. Soc. Japan* **21**, 201 (1966).

<sup>7</sup> D. K. Wohleben, Ph.D. thesis, University of California at San Diego, 1968 (unpublished).

<sup>8</sup> V. I. Chechernikov, I. Pop, and O. P. Naumkin, *Zh. Eksperim. i Teor. Fiz.* **44**, 1826 (1963) [English transl.: *Soviet Phys.—JETP* **17**, 1228 (1963)].

<sup>9</sup> W. E. Blumberg, J. Eisinger, V. Jaccarino, and B. T. Matthias, *Phys. Rev. Letters* **5**, 52 (1960).

<sup>10</sup> R. G. Barnes, F. Borsa, S. L. Segel, and D. R. Torgson, *Phys. Rev.* **137**, A1828 (1965).

<sup>11</sup> Y. Masuda, *J. Phys. Soc. Japan* **19**, 239 (1964).

<sup>12</sup> A. Narath and T. Fromhold, Jr., *Phys. Letters* **25A**, 49 (1967); A. Narath, *Phys. Rev.* **179**, 359 (1969).

<sup>13</sup> F. Y. Fradin, *Phys. Letters* **28A**, 441 (1968).

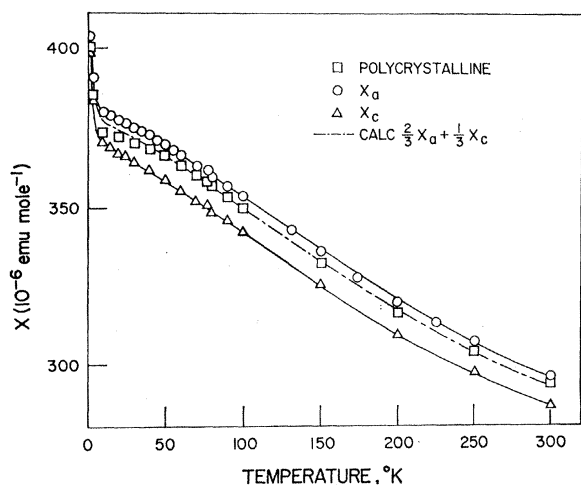


FIG. 1. Magnetic susceptibility  $\chi$  of scandium as a function of temperature.  $\chi_a$  and  $\chi_c$  are the susceptibilities of a scandium single crystal (ANL-IV) with the magnetic field parallel to the  $a$  axis and  $c$  axis, respectively. The polycrystalline data were obtained on the same material from which the single crystal was grown.

TABLE I. Mass spectrographic analyses for impurities in the scandium samples (factor-of-2 accuracy in ppm by weight).

Designation	KL-II	ANL-I	ANL-IV	Polycrystalline
Ag	10	100	1	0.5
Al	60	200	200	6
C				270
Ca	10	300	300	30
Cd		10		
Cu	200	40	20	40
Fe	40	100	100	50
K	10	30	30	0.4
Mg	0.7	20	20	5
Mn	0.1	30	0.3	0.15
Na	15	5	2	0.1
Nb		6		<0.06
Ni	10	10	1	4
P	1	2	2	1
Pb		6	3	9
Si	10	400	100	400-600
Ta	40	40		8
Th	500	50	2	5
Ti	1	3	3	5
Tl		6		
U			2	5
W		4		45
Zn		50	5	8
Y	6	2	20	65
Other nonrare earths	1	4	2	14
La	10	30	30	30
Ce	30	10	30	35
Pr	10	10	3	2
Nd	10	3	10	8
Sm	0.2	5	2	0.2
Gd	10	1	30	40
Tb	30	30	3	0.4
Hg	10	10	10	2
Ho	10	10	1	0.5
Er	10	4	10	10
Lu	1	0.4	4	3
Tm		1		0.1
Total rare earths	131.2	114.4	133	131.2
Total impurity	1046	1532.4	946.3	1202.4

anisotropy measurements were reported in a previous publication.<sup>14</sup>  $\chi_a - \chi_c$  was measured to within  $\pm 2 \times 10^{-9}$  emu  $g^{-1}$ . The NMR measurements were made by means of a pulsed NMR spectrometer that employed phase-coherent detection and a boxcar integrator. A bridge configuration was used with the single-crystal sample in one coil and a second coil for electrical balance. The NMR measurements were made at 8 MHz and at temperatures of 4.2 and 77°K. The single-crystal sample was oriented with the  $c$  axis normal to the axis of the rf coil. The orientation dependence was determined from measurements that were made with the magnetic field at various angles  $\theta$  with respect to the  $c$  axis. The anisotropic Knight shifts were measured relative to the powdered scandium metal. The  $T_1$  measurements were made either by using a  $\pi - \frac{1}{2}\pi$  pulse sequence for  $\theta \approx \cos^{-1}(1/\sqrt{3})$  or by using a saturating comb (50-100  $\frac{1}{2}\pi$  pulses) of about 20-msec duration. The anisotropic  $T_1$  measurements are reported for 77°K. The magnetic field was provided by a Varian 12-in. electromagnet; the rf field was about 140 Oe.

#### EXPERIMENTAL RESULTS

Figure 1 shows the magnetic susceptibility as a function of temperature for the polycrystalline scandium and the ANL-IV scandium single crystal. The weighted average susceptibility of the single crystal agrees very well with the polycrystalline sample. The susceptibility of the single crystal was measured with the magnetic field parallel to the  $a$  axis ( $\chi_a$ ) only, and the susceptibility with the magnetic field parallel to the  $c$  axis ( $\chi_c$ ) was deduced by combining the  $\chi_a$  susceptibility and the magnetic-anisotropy measurements. Also, the susceptibility of the ANL-IV single crystal

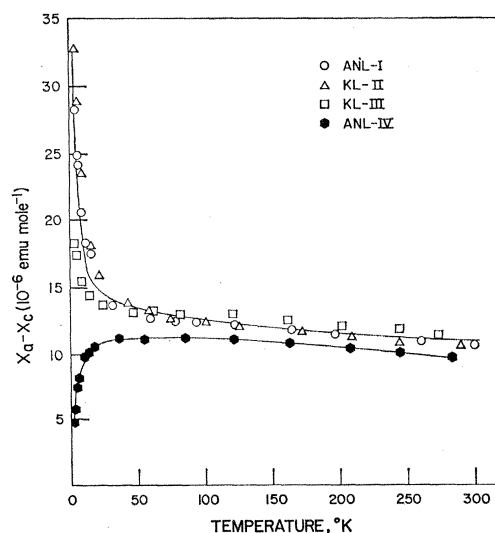


FIG. 2. Magnetic anisotropy (defined as the difference between  $\chi_a$  and  $\chi_c$ ) versus temperature for single crystals of scandium.

<sup>14</sup> J. W. Ross and D. J. Lam, Phys. Rev. **165**, 617 (1968).

was measured by Wohleben at the University of California at La Jolla, and the measurements made at both laboratories are in excellent agreement.

Figure 2 shows the difference in susceptibility between the  $a$  and  $c$  axis of the four single crystals. At high temperatures, the  $\chi_a - \chi_c$  values for all the crystals show a small temperature dependence but, at low temperatures, the ANL-IV crystal exhibits a different temperature dependence than the other three. The discrepancy is difficult to explain, especially between ANL-I and ANL-IV, since both crystals were prepared with the same starting material. Perhaps the arc- and levitation-melting techniques introduce different amounts of imperfections and impurities; however, any variations in the impurities of the two crystals must be within the accuracy of the spectroscopic analysis. It is important to point out the existence of a discrepancy between the results of this investigation and those reported earlier.<sup>8</sup> We found that the  $\chi_a$  is greater than  $\chi_c$ .

Figure 3 shows the amplitude of the Bloch decay following the last  $\frac{1}{2}\pi$  pulse as a function of pulse spacing for ANL-IV at 77°K and 8 MHz. The consistent straight-line plots indicate single exponential relaxation. The spin-lattice relaxation rate  $(T_1T)^{-1}$  at 77°K as a function of  $\sin^2\theta$ , where  $\theta$  is the angle between the  $c$  axis and the static magnetic field direction  $H_0$ , is shown in Fig. 4. There is a difference, by a factor of almost 2, in the relaxation rate between the  $a$  and  $c$  axes. At 4.2°K

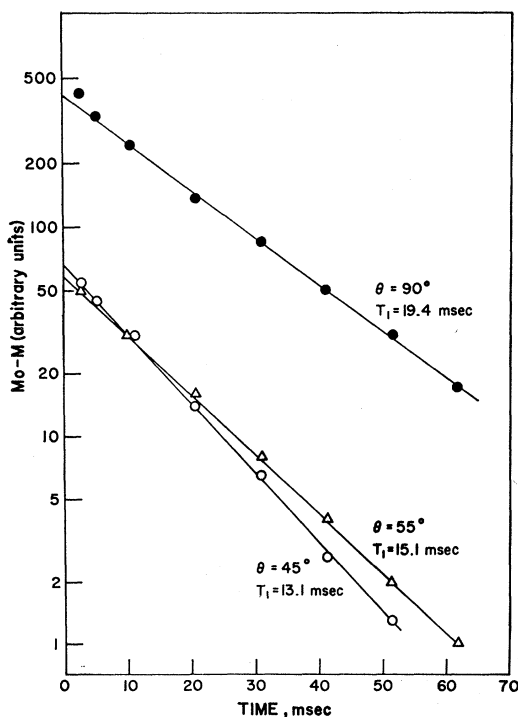


FIG. 3. Approach of the nuclear magnetization  $M$  to the thermal equilibrium value  $M_0$  as a function of time between the last saturating pulse and the  $\frac{1}{2}\pi$  measuring pulse. The data shown were taken at 77°K for various angles between the  $c$  axis and the static field direction.

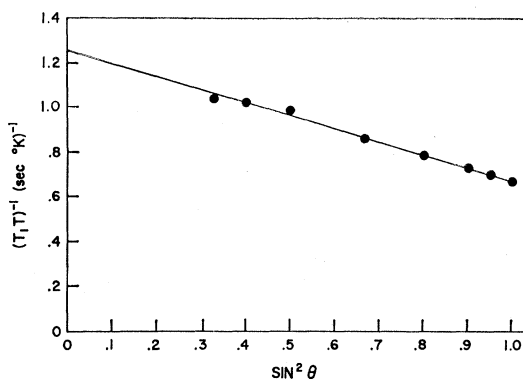


FIG. 4. Spin-lattice relaxation rate at 77°K as a function of the angle  $\theta$  between the  $c$  axis and the static field direction.

and 8 MHz, we find a value of  $T_1T = 1.1 \pm 0.1$  sec °K for  $\theta = \theta_0 = \cos^{-1}(1/\sqrt{3})$ . The value of  $T_1T$  at this angle corresponds to the powder-average value. Since at  $\theta_0$  the first-order quadrupole-split satellites collapse into the central transition, the resonance spectrum can be easily saturated. At 300°K and 12 MHz a value of  $T_1T = 1.2 \pm 0.1$  sec °K is found for a well-annealed polycrystalline sample by using a saturating comb (50-5- $\mu$ sec pulses) of 5-msec duration. The values of  $T_1T$  can be compared with the most recent value,  $T_1T = 1.3 \pm 0.2$  sec °K, reported by Narath.<sup>12</sup>

In order to obtain information about the nuclear electric-quadrupole interaction and the anisotropic Knight shifts, the first-order quadrupole-satellite splitting  $\delta H$  at 4.2°K and 8 MHz is plotted in Fig. 5 as a function of  $3 \cos^2\theta - 1$ . Here,  $\delta H$  is the splitting of the  $\frac{3}{2}, \frac{1}{2}$  and  $-\frac{1}{2}, -\frac{3}{2}$  satellites. The slope  $2\pi\nu_Q/\gamma$  of the linear plot of  $\delta H$  versus  $3 \cos^2\theta - 1$ , yields

$$\nu_Q = 3e^2qQ/2I(2I-1)\hbar = 0.124 \pm 0.004 \text{ MHz.}$$

Here  $\gamma$  is the gyromagnetic ratio of the nucleus,  $e$  is the charge of the electron,  $q$  is the electric field gradient,  $Q$  is the quadrupole moment of the scandium nucleus,  $I$  is the angular-momentum quantum number, and  $\hbar$  is Planck's constant. Barnes *et al.*<sup>10</sup> report a value of  $\nu_Q = 0.144 \pm 0.002$  MHz at room temperature for polycrystalline scandium.

The orientation-dependent Knight shift  $K(\theta)$  is given by  $K(\theta) = K_{ax}(3 \cos^2\theta - 1)$ , where  $\theta$  is the angle between the  $c$  axis and  $H_0$ . In Fig. 5,  $\Delta H = H_R K(\theta)$  is determined from  $\frac{1}{2}(H_{\frac{3}{2}, \frac{1}{2}} + H_{-\frac{1}{2}, -\frac{3}{2}}) - H_{\theta_0}$ , the midpoint between the positions of the  $\frac{3}{2}, \frac{1}{2}$  and  $-\frac{1}{2}, -\frac{3}{2}$  first-order quadrupole satellites relative to the midpoint at  $\theta = \theta_0$ . Here  $H_R$  is the resonance position of the powdered scandium. This method of determining  $K(\theta)$  avoids the angular dependence of the field position of the central transition due to the second-order quadrupolar effect. From the slope of the plot of  $\Delta H$  versus  $3 \cos^2\theta - 1$ , we obtained

$$\begin{aligned} K_{ax} &= -(0.032 \pm 0.002)\% \text{ at } 4.2^\circ\text{K} \\ &= -(0.030 \pm 0.002)\% \text{ at } 77^\circ\text{K}. \end{aligned}$$

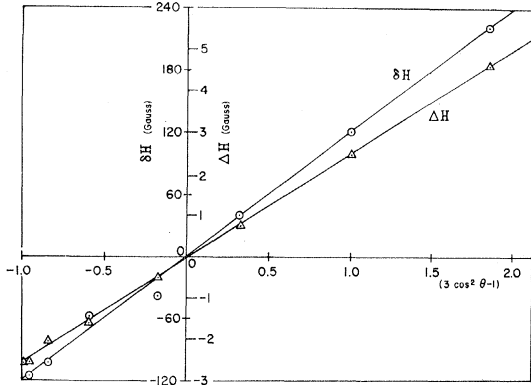


FIG. 5.  $\delta H$  is the splitting between the  $\frac{3}{2}, \frac{1}{2}$  and  $-\frac{1}{2}, -\frac{3}{2}$  satellites, plotted here as a function of the angle  $\theta$  between the  $c$  axis and the field direction.  $\Delta H$  is the shift of the midpoint of the satellite positions relative to the midpoint at  $\theta = \theta_0$ . Data taken at 4.2°K and 8 MHz.

If the  $K_{ax}$  value at 77°K is extrapolated to 300°K by using the change of  $\chi_a - \chi_c$  versus the temperature curve of ANL-IV in Fig. 2, the value at 300°K is consistent with the value  $K_{ax} = -(0.024 \pm 0.002)\%$  obtained by Barnes *et al.*<sup>10</sup> from measurements on a powdered scandium sample at room temperature.

## DISCUSSION

The important contributions to the observed relaxation rates in transition metals arise from core-polarization<sup>15</sup> and orbital<sup>16</sup> hyperfine interactions with the  $d$  component of the conduction-electron wave function at the Fermi level, as well as from the contact<sup>17</sup> hyperfine interaction with the  $s$  component. Conduction-electron contributions associated with magnetic-dipole<sup>16</sup> and electric-quadrupole<sup>18,19</sup> hyperfine interactions are usually quite small. Recently, Narath<sup>20</sup> discussed the strong dependence of the various contributions to the spin-lattice relaxation rate on the point-group symmetry properties of the  $d$  component of the conduction-electron wave function, i.e., the ratio of the  $A_1'$ ,  $E'$ , and  $E''$  orbital admixtures, in hcp metals. By means of the extreme tight-binding approximation, he developed a theory of spin-lattice relaxation in hcp crystals that predicts a field orientation dependence of the orbital contribution to the relaxation rate. The results of the angular dependence of the relaxation rates for scandium single crystals seems to substantiate his prediction. The discussion of our experimental results will follow the Narath theory closely, and we refer the reader to Narath's paper<sup>20</sup> for the details of the derivation and assumptions.

In the absence of  $s$ - $d$  mixing, spin-orbit coupling, and many-body enhancement effects, the spin-lattice relax-

ation rate  $R = (T_1 T)^{-1}$  can be expressed<sup>20</sup> as

$$R = \frac{4\pi}{\hbar} (\gamma_n \hbar)^2 k_B [N(0)]^2 \sum_i P_i^2 (K_i^{(1)} + K_i^{(2)} \sin^2 \theta), \quad (1)$$

where  $\gamma_n$  is the nuclear gyromagnetic ratio,  $k_B$  is the Boltzmann constant, and  $N(0)$  is the bare density of states at the Fermi level for *one* direction of spin. The sum is over the four hyperfine interactions:  $s$ -contact  $P_s = \rho H_{\text{hfs}}^s$ ,  $d$ -spin core-polarization  $P_d = (1 - \rho) H_{\text{hfs}}^d$ , and  $d$ -spin dipolar and  $d$ -orbital  $P_{\text{dip}} = P_{\text{orb}} = (1 - \rho) \times H_{\text{hfs}}^{\text{orb}}$ . Here  $\rho$  is the average fractional  $s$  character at the Fermi level,

$$\rho = N_s(0)/N(0).$$

The reduction factors  $K_i^{(1)}$  and  $K_i^{(2)}$  are given in analytic form by Narath<sup>20</sup> in terms of the parameters  $x$  and  $y$ , where

$$x = 2(F^{\Gamma(E')} + F^{\Gamma(E'')})(1 - \rho)^{-1} \quad (2a)$$

and

$$y = F^{\Gamma(E'')}(F^{\Gamma(E')} + F^{\Gamma(E'')})^{-1}. \quad (2b)$$

The  $F^{\Gamma(m)}$  terms are the average values of the fractional admixture coefficients at the Fermi level that have the same value for all  $m$ , which form a basis for a given irreducible representation  $\Gamma(m)$ :

$$F^{\Gamma(m)} = \sum_{\mu} \sum_k |C_{\mu mk}|^2 [\delta(E_{\mu k} - E_F)] [N(0)N]^{-1}, \quad (3)$$

where the  $C_{\mu mk}$  terms are the fractional admixture coefficients,  $E_{\mu k}$  is the energy of the electron with band index  $\mu$  and wave vector  $k$ ,  $E_F$  is the Fermi energy, and  $N(0)N$  is the total number of states per unit energy interval at the Fermi level for *one* direction of spin. An assumption of this treatment of spin-lattice relaxation is the neglect of the  $p$  admixture at the Fermi level [i.e.,  $N(0) = N_s(0) + N_d(0)$ ]. This is justified by the small  $p$  hyperfine field relative to that of the  $s$  electrons, and by the small  $p$  density of states at the Fermi surface relative to that of the  $d$  electrons.

The relevant point group for the hcp lattice is  $D_{6h}$ , which is a direct product group  $D_{6h} = D_{3h} \times I$ . The hcp lattice contains two atoms per unit cell, which are related by the operations of the space group  $P6_3/mmc$ . Since the nuclear-resonance properties of the two non-equivalent atoms are identical, the treatment may be limited to a primitive lattice with  $D_{3h}$  point-group

TABLE II. Irreducible representation about the point  $\Gamma$  in the Brillouin zone of the hcp lattice.

Bases	$l=0, 1, \text{ and } 2$ harmonics <sup>a</sup>
$A_1'$	$Y_0^0, Y_2^0$
$A_2''$	$Y_1^0$
$E'$	$Y_1^{1,c}, Y_1^{1,s}$
	$Y_2^{2,c}, Y_2^{2,s}$
$E''$	$Y_2^{1,c}, Y_2^{1,s}$

<sup>a</sup>  $Y_{l^m,s} = (Y_l^m + Y_l^{-m})/\sqrt{2}$ ;  $Y_{l^m,s} = -i(Y_l^m - Y_l^{-m})/\sqrt{2}$ .  $Y_l^m = Y_l^m(\alpha, \beta)$  are normalized spherical harmonics. The polar angle  $\alpha$  is measured with respect to a  $z$  axis parallel to the crystallographic  $c$  axis.

<sup>15</sup> Y. Yafet and V. Jaccarino, Phys. Rev. **133**, A160 (1964).

<sup>16</sup> Y. Obata, J. Phys. Soc. Japan **18**, 1020 (1963).

<sup>17</sup> J. Korringa, Physica **16**, 601 (1950).

<sup>18</sup> A. H. Mitchell, J. Chem. Phys. **26**, 1714 (1957).

<sup>19</sup> Y. Obata, J. Phys. Soc. Japan **19**, 2348 (1964).

<sup>20</sup> A. Narath, Phys. Rev. **162**, 320 (1967).

TABLE III. Range of allowable solutions for the reduction factors and orbital admixture coefficients.

$x$	$y$	$K_{\text{orb}}^{(1)}$	$K_{\text{orb}}^{(2)}$	$K_d^{(1)}$	$K_{\text{dip}}^{(1)}$	$K_{\text{dip}}^{(2)}$	$F\Gamma(E')^a$	$F\Gamma(E'')^a$	$K_{\text{orb}}^{(1)}/K_{\text{orb}}^{(2)}$
0.301	1.00	0.631	-0.293	0.534	0.0176	0.0148	0.00	15.05	-2.155
0.153	1.00	0.389	-0.189	0.729	0.0178	0.0225	0.00	7.65	-2.062
0.259	0.925	0.537	-0.254	0.579	0.0187	0.0163	0.97	11.98	-2.114
0.317	0.875	0.579	-0.269	0.505	0.0200	0.0129	1.98	13.87	-2.155
0.180	0.875	0.391	-0.189	0.685	0.0193	0.0200	1.12	7.87	-2.071
0.284	0.800	0.501	-0.234	0.540	0.0211	0.0138	2.84	11.36	-2.138
0.258	0.682	0.406	-0.189	0.569	0.0229	0.0140	4.10	8.80	-2.153

<sup>a</sup> In units of  $10^{-2}(1-\rho)$ .

symmetry. The appropriate decomposition<sup>21</sup> of the  $l=0, 1$ , and 2 representation of the three-dimensional rotation group leads to symmetry functions; angular parts are presented in Table II in terms of normalized spherical harmonics  $Y_l^m(\alpha, \beta)$ . The polar angle  $\alpha$  is measured with respect to a  $z$  axis parallel to the crystallographic  $c$  axis.

In the extreme tight-binding limit, the  $s$ - $d$  interactions have no effect on the relaxation rate for cubic metals, since the  $s$  and  $d$  functions belong to different irreducible representations of the cubic point group. However, reference to Table II shows that both  $s(Y_0^0)$  and  $d(Y_2^0)$  belong to the  $A_1'$  representation of  $D_{3h}$  in the hexagonal case. Hence, matrix elements of the contact and core-polarization interactions will interfere, provided these functions are admixed in the conduction-electron wave functions  $\Psi(\mathbf{r})$  at the Fermi surface. If the  $A_1'$  functions are expressed as linear combinations of the form

$$\xi_{\mu k} Y_0^0 + (1 - \xi_{\mu k}^2)^{1/2} Y_2^0,$$

the resulting interference term is

$$R_{s-d} = (8\pi/\hbar)(\gamma_n \hbar)^2 k_B [N(0)]^2 H_{\text{hfs}}^{(s)} H_{\text{hfs}}^{(d)} \times \langle (F_{\mu k} \Gamma^{(A_1')})^2 \xi_{\mu k}^2 (1 - \xi_{\mu k}^2) \rangle_{\mathbf{E}_F}, \quad (4)$$

where the term in the angular brackets is an average over the Fermi surface. Since  $H_{\text{hfs}}^{(s)}$  and  $H_{\text{hfs}}^{(d)}$  are of opposite sign ( $H_{\text{hfs}}^{(d)} < 0$ ), this term interferes destructively with Eq. (1).

The orientation-dependent relaxation-rate equation derived from Fig. 4 for the ANL-IV single crystal can be expressed in the form

$$R = 1.25 - 0.58 \sin^2 \theta (\text{sec } ^\circ\text{K})^{-1}. \quad (5)$$

Since the  $s$ -contact and  $d$ -spin core-polarization terms are isotropic, we set

$$-0.58 (\text{sec } ^\circ\text{K})^{-1} = (4\pi/\hbar)(\gamma_n \hbar)^2 k_B [N(0)]^2 \times [(1-\rho)H_{\text{hfs}}^{\text{orb}}]^2 K^{(2)}. \quad (6a)$$

The reduction factor  $K^{(2)}$  consists of the  $d$ -orbital and  $d$ -spin dipolar contributions. Since the isotropic term in Eq. (5) consists of  $s$ -contact,  $d$ -spin core-polarization, and dipolar contributions in addition to the orbital contribution, Eq. (5) sets an upper limit for the ratio

of  $K_{\text{orb}}^{(1)}$  and  $K_{\text{orb}}^{(2)}$ :

$$K_{\text{orb}}^{(1)}/-K_{\text{orb}}^{(2)} \leq 2.155. \quad (6b)$$

A lower limit of 0.189 on  $-K_{\text{orb}}^{(2)}$  is determined from Eq. (6a) and the measured electronic specific-heat coefficient. This limit is discussed in the latter part of this section. By using the two limits and Eqs. (2.30)–(2.37) of Narath<sup>20</sup> for the functional forms of the  $K_i$ , a range of permissible values for the orbital admixture parameters  $x$  and  $y$  can be obtained as shown on the crosshatched area of Fig. 6. Table III lists the range of allowable solutions for  $x$  and  $y$  and the other parameters calculated from these values of  $x$  and  $y$ .

We can estimate the amount of dipolar contribution to the relaxation rate by setting

$$R_{\text{orb}}^{(2)}/R_{\text{dip}}^{(2)} = K_{\text{orb}}^{(2)}/K_{\text{dip}}^{(2)}$$

and

$$R_{\text{orb}}^{(1)}/R_{\text{dip}}^{(1)} = K_{\text{orb}}^{(1)}/K_{\text{dip}}^{(1)},$$

within the range of permissible values for  $x$  and  $y$ . We find that the anisotropic dipolar contribution is only

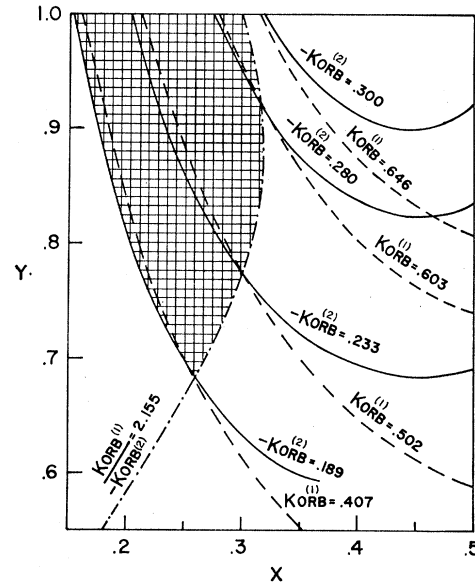


FIG. 6. Allowable range of the orbital admixture parameters  $x$  and  $y$  is indicated by the crosshatched area. The boundary  $K_{\text{orb}}^{(1)}/K_{\text{orb}}^{(2)} = -2.155$  set by the ratio of the angular-independent to the angular-dependent relaxation rate in Eq. (5) is shown. Also shown are various pairs of lines of constant  $K_{\text{orb}}^{(1)}$  and  $K_{\text{orb}}^{(2)}$  satisfying the above equality.

<sup>21</sup> S. L. Altmann and C. J. Bradley, Rev. Mod. Phys. 37, 33 (1965).

about 4–8% of the anisotropic orbital contribution, and the isotropic dipolar part of the relaxation is about 2–5% of the isotropic orbital-relaxation rate.

We may estimate the quadrupolar contribution to the relaxation rate from the following ratio<sup>19</sup>:

$$\frac{R_Q}{R_{\text{dip}}} = \frac{(e^2 Q_{\text{eff}})^2}{(\gamma_e \gamma_n \hbar^2 I)^2} \frac{3(2I+1)}{10(2I-1)},$$

where  $Q_{\text{eff}}$  is the effective quadrupole moment of the scandium nucleus and  $\gamma_e$  is the electron gyromagnetic ratio.  $Q_{\text{eff}}$  may differ from  $Q_{\text{Sc}}$  because of antishielding effects.<sup>22</sup> In metals these effects are probably quite small,<sup>23</sup> and we thus take  $Q_{\text{eff}} = Q_{\text{Sc}} = 0.22 \times 10^{-24}$  cm<sup>2</sup>, and find

$$R_Q/R_{\text{dip}} = 0.14.$$

Therefore, the quadrupolar contribution to the relaxation rate is probably less than 1% of the orbital contribution. Based on these estimates, the dipolar and the quadrupolar contributions to the relaxation rate will be ignored in the remainder of the paper. The error introduced by ignoring these two contributions will be less than 10% for  $K^{(2)}$  and less than 6% for  $K^{(1)}$ .

We substitute  $K_{\text{orb}}^{(2)}$  for  $K^{(2)}$  in Eq. (6a) and use the range of values of  $K_{\text{orb}}^{(2)}$  from  $-0.189$  to  $-0.293$  (see Fig. 6 and Table III) to obtain (in cgs units),

$$2.58 \times 10^{34} \leq [N(0)(1-\rho)H_{\text{hfs}}^{(\text{orb})}]^2 \leq 4.0 \times 10^{34}. \quad (7)$$

The lower limit is given by the largest value of  $K_{\text{orb}}^{(2)}$  that satisfies  $K_{\text{orb}}^{(1)}/-K_{\text{orb}}^{(2)} \leq 2.155$ . The upper limit of Eq. (7) is determined from  $K_{\text{orb}}^{(2)} = -0.189$ .

The orbital hyperfine field per unit orbital angular momentum is given, to a good approximation, by  $H_{\text{hfs}}^{(\text{orb})} = 2 \mu_B \langle r^{-3} \rangle$ , where  $\langle r^{-3} \rangle$  represent an average over the radial distribution of the  $d$  electrons near the Fermi surface. If we take the  $\text{Sc}^{2+}(3d^1)$  free-ion value<sup>24</sup> of  $\langle r^{-3} \rangle$  and multiply by  $\frac{3}{4}$  to obtain the approximate value in the metal,  $\langle r^{-3} \rangle_{\text{metal}} = 0.80 \times 10^{25}$  cm<sup>-3</sup>, then  $H_{\text{hfs}}^{(\text{orb})} = 0.148 \times 10^6$  Oe. From Eq. (7) we can write

$$1.086 \times 10^{12} \leq N(0)(1-\rho) \leq 1.353 \times 10^{12}, \quad (8)$$

where the unit for  $N(0)$  is states erg<sup>-1</sup> atom<sup>-1</sup>. The measured electronic specific-heat coefficient<sup>25</sup>  $\gamma$  for the scandium we studied is 10.34 mJ deg<sup>-2</sup> mole<sup>-1</sup>, and the density of states per spin  $N_\gamma(0)$  derived from the  $\gamma$  value is  $1.353 \times 10^{12}$  states erg<sup>-1</sup> atom<sup>-1</sup>. Our choice of  $-K_{\text{orb}}^{(2)} \geq 0.189$ , following Eq. (6), is to restrict the product  $N(0)(1-\rho)$  to a value less than or equal to the experimental value of  $N_\gamma(0)$ . The upper limit in Eq. (8) is valid, since the value of  $N_\gamma(0)$  is usually larger than the bare density of states in transition metals

<sup>22</sup> R. Sternheimer, Phys. Rev. **84**, 244 (1951).

<sup>23</sup> A. Narath and D. W. Alderman, Phys. Rev. **143**, 328 (1966).

<sup>24</sup> A. J. Freeman and R. E. Watson, in *Magnetism*, edited by G. T. Rado and H. Suhl (Academic Press Inc., New York, 1965), Vol. IIA.

<sup>25</sup> H. E. Flotow and D. W. Osborne (to be published).

because of the electron-electron, electron-phonon, and electron-paramagnon enhancement effects.

It is quite clear from Eq. (8) that only a limited range of  $N(0)$  and  $\rho$  can be used to account for the experimental relaxation rate. If the value of  $\rho$  is assumed to be zero, which is an unlikely event, the range of  $N(0)$  for one direction of spin is between 1.732 to 2.165 states eV<sup>-1</sup> atom<sup>-1</sup>. But if a reasonable value,  $\rho = 0.1$ , is taken, then the range of  $N(0)$  narrows to between 1.93 and 2.165 states eV<sup>-1</sup> atom<sup>-1</sup>. It should be pointed out that within the limits of Eq. (8),  $\rho$  cannot be greater than 0.112. The derived values of  $N(0)$  and  $\rho$  have not considered the experimental uncertainty, the errors introduced by ignoring the  $K_{\text{dip}}$  terms, and the estimate of  $H_{\text{hfs}}^{\text{orb}}$ . However, the inclusion of these possible errors would change the lower limit of  $N(0)$  and the upper limit of  $\rho$  by about 30%, i.e.,  $N(0) \gtrsim 1.4$  states eV<sup>-1</sup> atom<sup>-1</sup> and  $\rho \lesssim 0.15$ . Recently, Fleming and Loucks<sup>26</sup> derived a  $N(0)$  value of about 1.1 states eV<sup>-1</sup> atom<sup>-1</sup> for hcp scandium by the APW method. Their value of  $N(0)$  is about twice as large as that derived by Altmann and Bradley,<sup>27</sup> but is close to our lower limit.

The lowest ratio of  $K_{\text{orb}}^{(1)}/K_{\text{orb}}^{(2)}$ , as shown in Table III, is  $-2.062$  and is only about 5% lower than the limit of 2.155. This means that the observed total-relaxation rate may be approximately accounted for by the orbital term alone. In other words, we may set

$$R_s + R_d + R_{s-d} = 0,$$

$$\rho^2 (H_{\text{hfs}}^{(s)})^2 + K_d^{(1)} (1-\rho)^2 (H_{\text{hfs}}^{(d)})^2 + 2H_{\text{hfs}}^{(s)} H_{\text{hfs}}^{(d)} \times \langle F_{\mu k}^{\Gamma(A_1')} \xi_{\mu k}^2 (1 - \xi_{\mu k}^2) \rangle_{\mathcal{E}_F} = 0. \quad (9a)$$

By using the range of values of  $K_d^{(1)}$  from Table III, and by assuming that  $\rho = 0.02$  to 0.15 and  $H_{\text{hfs}}^{(d)}/H_{\text{hfs}}^{(s)} = -10^{-1}$ , the percentage admixture of  $s(Y_0^0)$  into the  $A_1'$  functions at the Fermi surface can be estimated. We obtained

$$\langle (F_{\mu k}^{\Gamma(A_1')})^2 \xi_{\mu k}^2 (1 - \xi_{\mu k}^2) \rangle_{\mathcal{E}_F} = 0.03 \text{ to } 0.16. \quad (9b)$$

Since  $\sum_m F^{\Gamma(m)} = 1$ , we made use of the values of  $F^{\Gamma(E')}$  and  $F^{\Gamma(E'')}$  in Table III and Eq. (9b) to estimate the range of  $\xi_{\mathcal{E}_F}^2$  from 5 to 22%. An alternative approach is to again assume that we can average the factors in the pointed bracket in Eq. (9a) separately and make the substitution  $\rho = \xi_{\mathcal{E}_F}^2 F^{\Gamma(A_1')}$ . We may then make use of the values of  $K_d^{(1)}$  and of  $F^{\Gamma(E')}$  and  $F^{\Gamma(E'')}$  in Table III. The latter two quantities are also functions of  $(1-\rho)$ . With the above-stated substitutions, Eq. (9a) is quadratic in  $\rho$  and may be solved for various values of  $H_{\text{hfs}}^{(d)}/H_{\text{hfs}}^{(s)}$ . For  $H_{\text{hfs}}^{(d)}/H_{\text{hfs}}^{(s)}$  between  $-0.05$  and  $-0.2$ ,  $\rho$  has values between 2.4 and 7.3% and  $\xi_{\mathcal{E}_F}^2$  has values between 3.0 and 11.2%. Thus, we can account for the rather small relaxation rate in scandium by recognizing the importance of the  $s$ - $d$  interference term. We have shown that a relatively small admixture

<sup>26</sup> G. S. Fleming and T. L. Loucks, Phys. Rev. **173**, 685 (1968).

<sup>27</sup> S. L. Altmann and C. J. Bradley, Proc. Phys. Soc. (London) **92**, 64 (1967).

(2.4–7.3%) of  $s$  character at the Fermi surface, which is well within our previous estimate of 0–15%, is consistent with the experimental relaxation rate.

We have consciously ignored effects of electron-electron<sup>28,29</sup> and electron-paramagnon<sup>30</sup> enhancement on  $T_1$ , because the relaxation rate is well accounted for by the orbital hyperfine interaction. Either enhancement effect is spin-coupled and would only enter the orbital relaxation rate via spin-orbit coupling, which is probably small in scandium. In the absence of spin-orbit coupling, electron-electron and electron-paramagnon enhancement would enter the isotropic relaxation rate through  $R_s$  and  $R_d$  as well as through  $R_{s-d}$ . Our experimental results, however, indicate that the sum  $R_s + R_d + R_{s-d}$  is approximately equal to zero.

We now turn to a discussion of the anisotropic Knight shift and its relation to the anisotropic susceptibility. The anisotropic Knight-shift results do not show as drastic a decrease in magnitude as the anisotropic susceptibility, measured on the same ANL-IV sample, from 77 to 4.2°K. The large change in anisotropy observed in the bulk magnetization is probably caused by a localized magnetic-impurity effect. (This point will be discussed by the authors in a paper now in preparation.) The impurities do not affect the majority of scandium nuclei, since the magnetic-impurity content is only about 100 ppm. Thus, the Sc<sup>45</sup> anisotropic Knight shift is probably a correct measure of the “pure” scandium magnetic anisotropy at low temperature, i.e., there is probably only a gradual increase in the magnitude of the anisotropy from 77 to 4.2°K, amounting to only about a 6% increase in  $\chi_a - \chi_c$  at 4.2°K.

In the absence of spin-orbit coupling, we will consider two contributions to  $K_{ax}$ , namely, the orbital contribution  $K_{ax}^{vv}$  and the spin-dipolar contribution  $K_{ax}^{dip}$ . If we assume that the anisotropic susceptibility  $\chi_a - \chi_c$  above 77°K is entirely of the Van Vleck orbital type,<sup>31</sup> we can write

$$\frac{1}{3}(K_c^{vv} - K_a^{vv}) = K_{ax}^{vv} = 2\langle r^{-3} \rangle \left[ \frac{1}{3}(\chi_c - \chi_a) \right] N^{-1}. \quad (10)$$

It should be emphasized<sup>32</sup> that the value of  $\langle r^{-3} \rangle$  to be used in the orbital Knight shift differs from the value that enters into orbital relaxation; the former is to be averaged over all occupied states of the  $d$  band, whereas the latter involves only the average over states at the Fermi level. Taking the 77°K value of  $\chi_a - \chi_c = 11.2 \times 10^{-6}$  emu/mole and using the estimate employed in the  $T_1$  calculation  $\langle r^{-3} \rangle_{\text{metal}} = 0.80 \times 10^{25} \text{ cm}^{-3}$ , we find that  $K_{ax}^{vv} = -0.01\%$ , a value that is a factor of 3 smaller in magnitude than the experimental value of  $-0.030\%$ . This difference may reflect the fact that additional spin contributions can contribute to  $\chi_c - \chi_a$ ,

if the effective-mass tensor is anisotropic, as would be expected for scandium.

To estimate the spin-dipolar contribution to  $K_{ax}$ , we follow the treatment of Boon.<sup>33</sup> His treatment leads to

$$K_{ax}^{dip} = -\frac{1}{2} \int d^3r' \frac{F'(r')}{r'^3} P_2^0(\cos\theta'), \quad (11)$$

with

$$F'(r') = g^2 \mu_B^2 \sum_k \left( \frac{\partial f}{\partial E_k} \right) |\psi_k(r')|^2. \quad (12)$$

Here  $P_2^0(\cos\theta')$  is an associated Legendre polynomial,  $\psi_k(r')$  are eigenfunctions of the electron Hamiltonian,  $g$  is the usual electron magnetic moment assumed equal to two for our case,  $\mu_B$  is the Bohr magneton, and  $f$  is the Fermi function.

It is clear from the orthogonality of the Legendre polynomials that the angular part of  $F'(r')$  must transform as  $P_2^0$  for  $K_{ax}^{dip}$  to be nonvanishing. For purposes of our estimate, we will ignore the cross terms in  $|\psi_k(r')|^2$  derived from a product of  $l=1$  functions. For a transition metal, the  $s-d$  cross terms, which transforms as  $P_2^0(\cos\theta)$ , will be of more interest. The contribution to  $K_{ax}^{dip}$  from these terms is given by

$$K_{ax}^{dip} = (1/\sqrt{5}) g^2 \mu_B^2 N(0) \langle r_{s-d}^{-3} \rangle_{EF} \times \langle F_{\mu k}^{\Gamma(A_1')} \xi_{\mu k} (1 - \xi_{\mu k}^2)^{1/2} \rangle_{EF}, \quad (13)$$

where

$$\langle r_{s-d}^{-3} \rangle_{EF} = \int \frac{\langle R_{4s}(r') R_{3d}(r') \rangle_{EF}}{r'^3} r'^2 dr'. \quad (14)$$

In order to estimate  $\langle r_{s-d}^{-3} \rangle_{EF}$ , we have carried out the analogous atomic integral for  $\langle r_{s-d}^{-3} \rangle$  using Herman-Skillman<sup>34</sup> wave functions for scandium  $3d$  and  $4s$  electrons. If we employ Eq. (13) and our earlier estimates of  $N(0)$ ,  $\xi_{EF}$ , and  $F^{\Gamma(A_1')}$ , we find that  $K_{ax}^{dip}$  is only about 8% of  $K_{ax}^{vv}$ .

It is possible to estimate the contribution of the Van Vleck orbital susceptibility  $\chi_{vv}$  to the total susceptibility of a powder from the orbital admixture coefficients in Table III and the measured value of  $\chi_a - \chi_c$ . The form of  $\chi_{vv}$  has been given by Kubo and Obata<sup>35</sup> as

$$\chi_{vv} = \mu_B^2 \sum_{nn'} \int \frac{d\mathbf{k}}{(2\pi)^3} \left( \frac{f(E_n(\mathbf{k})) - f(E_{n'}(\mathbf{k}))}{E_{n'}(\mathbf{k}) - E_n(\mathbf{k})} \right) \times \langle n\mathbf{k} | \mathbf{L} | n'\mathbf{k} \rangle \langle n'\mathbf{k} | \mathbf{L} | n\mathbf{k} \rangle, \quad (15)$$

where  $n$  and  $n'$  are band indices,  $f(E_n(\mathbf{k}))$  is the Fermi function at the energy  $E_n(\mathbf{k})$ , and  $\mathbf{k}$  is the wave vector. Here,  $\mathbf{L}$  is the angular-momentum operator.

Let us define the matrix elements

$$L_\alpha \equiv \langle n\mathbf{k} | L_\alpha | n'\mathbf{k} \rangle \quad (16)$$

<sup>28</sup> Y. Moriya, J. Phys. Soc. Japan **18**, 516 (1963).

<sup>29</sup> A. Narath and H. T. Weaver, Phys. Rev. **175**, 373 (1968).

<sup>30</sup> S. Doniach, J. Appl. Phys. **39**, 483 (1968).

<sup>31</sup> A. M. Clogston, V. Jaccarino, and Y. Yafet, Phys. Rev. **134**, A650 (1964).

<sup>32</sup> Y. Yafet and V. Jaccarino, Phys. Rev. **133**, A1630 (1964).

<sup>33</sup> M. H. Boon, Physica **30**, 1326 (1964).

<sup>34</sup> F. Herman and S. Skillman, *Atomic Structure Calculations* (Prentice-Hall, Inc., Englewood Cliffs, N. J., 1963).

<sup>35</sup> R. Kubo and Y. Obata, J. Phys. Soc. Japan **11**, 547 (1956).

(where  $\alpha$  is the direction parallel or perpendicular to the  $c$  axis for  $L_{11}$  and  $L_{\perp}$ , respectively) and focus our attention on the  $d$ -like functions using the representations of Table II. Then we have

$$L_{11} = \sum_{mm'} |C_{mnk}|^2 |C_{m'n'k}|^2 |\langle m' | L_z | m \rangle|^2, \quad (17)$$

with the notation used earlier,

$$L_{11} = 8 |C_{E'nk}|^2 |C_{E'n'k}|^2 + 2 |C_{E''nk}|^2 |C_{E''n'k}|^2. \quad (18)$$

Also,

$$L_{\perp} = \frac{1}{2} (6 |C_{A_1'nk}|^2 |C_{E''n'k}|^2 + 4 |C_{E'nk}|^2 |C_{E''n'k}|^2 + 6 |C_{E'nk}|^2 |C_{A_1'n'k}|^2 + 4 |C_{E''nk}|^2 |C_{E'n'k}|^2). \quad (19)$$

Since the major contribution to  $\chi_{vv}$  [Eq. (15)] arises from states with  $|E_{n'}(k) - E_n(k)|$  at a minimum, that is, states near the Fermi level, we will average the coefficients according to Eq. (3). Then we have

$$L_{11} = 8 [E^{\Gamma(E')}]^2 + 2 [F^{\Gamma(E'')}]^2 \quad (20)$$

and

$$L_{\perp} = 6 F^{\Gamma(A_1')} F^{\Gamma(E'')} + 4 F^{\Gamma(E'')} F^{\Gamma(E')}. \quad (21)$$

Regardless of the value of  $\rho$  that is used, it is clear from the experimentally determined values of the  $F^{\Gamma}$ 's in Table III that Eqs. (20) and (21) indicate that  $\chi_a$  is greater than  $\chi_c$ . This is consistent with our magnetic-susceptibility and magnetic-anisotropy measurements, but is opposite to the previous results obtained by Chechernikov *et al.*<sup>3</sup> Again taking the values of  $F^{\Gamma}$  from Table III, the ratio of the differential susceptibility to the powder susceptibility that results from the Van Vleck mechanism may be estimated from

$$(\chi_a - \chi_c) / \chi_{\text{powder}} = (L_{\perp} - L_{11}) / (\frac{2}{3} L_{\perp} + \frac{1}{3} L_{11}).$$

This ratio is on the order of 1.4. If it is assumed that the differential susceptibility, equal to  $11.2 \times 10^{-6}$  emu/mole at 77°K, is entirely of the Van Vleck type, then the Van Vleck contribution to the susceptibility of the powder sample is estimated to be only about  $8 \times 10^{-6}$  emu/mole. This value is an order of magnitude smaller than the previous estimated value of about  $100 \times 10^{-6}$  emu/mole for scandium.<sup>5</sup> The measured magnetic susceptibility ( $370 \times 10^{-6}$  emu/mole) is the sum of the Pauli susceptibility of the  $s$  and  $d$  electrons, the diamagnetism of the ion core and the conduction electrons, and the orbital paramagnetism. By using the estimated value of  $\chi_{\text{orb}}$  ( $10^{-5}$  emu/mole) and  $\chi_{\text{diam}}$  ( $-10^{-5}$  emu/mole), an

enhancement factor of about 3.5 for the spin susceptibility is obtained relative to our determination of the bare density of states,  $N(0)$ . (See note added in proof.)

## SUMMARY

The results of the present investigation on scandium can be summarized as follows:

(1) The magnetic susceptibility parallel to the  $a$  axis is greater than that parallel to the  $c$  axis.

(2) The nuclear spin-lattice relaxation rate in scandium can be attributed almost totally to the orbital hyperfine interaction. From the results of the spin-lattice relaxation rate on single-crystal scandium, the upper and lower limits have been derived for the average fractional  $s$ -electron character at the Fermi surface (2.4–15%), the electronic density of states at the Fermi surface (1.4–2.16 states  $\text{eV}^{-1}$  atom $^{-1}$  per spin), and the average fractional admixture coefficients at the Fermi surface.

(3) The cancellation of the  $s$ -contact and  $d$ -spin core-polarization terms by the  $s$ - $d$  cross term in the relaxation rate is evidence for the presence of  $s$ - $d$  mixing at the Fermi level. The presence of hybridized  $s$  and  $d$  bands at the Fermi level is consistent with the experimental results that  $dK/dX > 0$ ,<sup>5,9,10</sup> and with recent theoretical calculations<sup>26</sup> of the band structure of scandium.

(4) The orbital paramagnetism for scandium has been estimated as about  $10 \times 10^{-6}$  emu/mole, which is an order of magnitude smaller than the estimated value of  $100 \times 10^{-6}$  emu/mole reported by earlier investigators.

*Note added in proof.* The absence of superconductivity in scandium can be understood by the small enhancement of  $N_{\gamma}(0)$  over  $N(0)$ , i.e., a small electron-phonon interaction. Using the values of  $N_x(0)$ ,  $N_{\gamma}(0)$ , and  $N(0)$ , we estimate an upper limit for the superconducting transition temperature of about  $10^{-3}$ °K.

## ACKNOWLEDGMENTS

The valuable assistance of R. Panosh, J. Pasteris, and J. Downey with the experiments is gratefully acknowledged. We wish to thank Dr. A. J. Freeman, Dr. W. E. Gardner, Dr. I. Goroff, Dr. F. M. Mueller, and Dr. T. J. Rowland for helpful discussions. The cooperation of Dr. D. K. Wohlleben of the University of California at La Jolla is also gratefully appreciated.